Journal of Thermal Analysis and Calorimetry, Vol. 74 (2003) 895–904

ZINC(II)DI(*o*-HYDROXYBENZOATE) COMPLEXES WITH IMIDAZOLE AND ITS DERIVATIVES
Synthesis, thermal characterization and molecular structures

M. Olczak-Kobza[*], *R. Czylkowski and J. Karolak-Wojciechowska*

Institute of General and Ecological Chemistry, Technical University, 90–924 Łódź, Poland

(Received November 29, 2002; in revised form July 22, 2003)

Abstract

Mixed complexes of the type: $Zn(Hsal)_2(Him)_2$, $Zn(Hsal)_2(Him)_5$, $Zn(Hsal)_2(4\text{–}MeHim)_2$ and $Zn(Hsal)_2(1,2\text{-}diMeim)_2$ (where *Hsal*=$OHC_6H_4COO^-$, *Him*=imidazole, 4-*MeHim*=4-methylimidazole, 1,2-*diMeim*=1,2-dimethylimidazole) have been synthesized. The application of chemical, thermal and X-ray methods has enabled us to analyze the complexes and their sinters. The gaseous products of pyrolysis of $Zn(Hsal)_2(Him)_2$ and $Zn(Hsal)_2(4\text{–}MeHim)_2$ have been investigated. Thermal decomposition pathways have been postulated for synthesized complexes. The molecular structures of the $Zn(Hsal)_2(Him)_2$ and $Zn(Hsal)_2(1,2\text{-}diMeim)_2$ have been solved.

Keywords: heteroligand complexes, *o*-hydroxybenzoic acid, thermal analysis, zinc(II), X-ray structures

Introduction

The present work is a continuation of our studies on the synthesis and properties of zinc(II) and cadmium(II) heteroligand complexes. Organic ligands of the H_2L type (such as: *o*-hydroxybenzoic acid, *o*-aminobenzoic acid, *o*-hydroxybenzaldoxime) and bivalent metals form either di-complexes $M(HL)_2$ or mono-complexes ML (where *M*=metal ion, *HL*=$OHC_6H_4COO^-$, $NH_2C_6H_4COO^-$, $OC_6H_4CHNOH^-$, *L*=$OC_6H_4COO^{2-}$, $NHC_6H_4COO^{2-}$, $OC_6H_4CHNO^{2-}$). The mono-compounds may bind to the other monodentate ligands [1, 2] as well as to bidentate [3–5], whereas the di-compounds – only to monodentate ones [4].

The complexes of zinc(II) with imidazole and its derivatives have been investigated in the solid-state as well as in the solution for a long time now [6–8]. In the molecule of imidazole, nitrogen N3 occupies a preference place of the coordination and the property of coordination is determined by the type and position of the substituent in the ring. The methyl group decreases the complexing power in the following order: imidazole>4-methylimidazole>1,2-dimethylimidazole [7].

---

[*] Author for correspondence: E-mail: wkobza@p.lodz.pl

1388–6150/2003/ $ 20.00

Akadémiai Kiadó, Budapest
Kluwer Academic Publishers, Dordrecht

Zinc(II) forms simple as well as mixed complexes with imidazole (or its derivatives) and e.g. with aliphatic and amino acid [9–12]. In analogous surroundings, zinc occurs in important biological molecules (metalloproteins and metalloenzymes) and, therefore, complexes containing such ligands are frequently researched by means of the spectroscopic, structural, and thermal investigation [11–13].

The investigations of these complexes in solution provide the important information about properties of biologically active molecules and the investigations in the solid-state are complemented. Recently, we have prepared new zinc complexes with aromatic acids and imidazoles of general formulas: $Zn(Hsal)_2(Him)_2$, $Zn(Hsal)_2(Him)_5$, $Zn(Hsal)_2(4\text{-}MeHim)_2$ and $Zn(Hsal)_2(1,2\text{-}diMeim)_2$. Structure and thermal characteristic of these complexes have been determined.

Experimental

Materials

P.a.: $ZnCO_3$, *o*-hydroxybenzoic acid, ethanol (POCh – Gliwice), imidazole (Fluka Chemie AG), 4-methylimidazole, 1,2-dimethylimidazole (Sigma) were used without additional purification.

Preparation

Zinc di(*o*-hydroxybenzoate) was obtained according to the method described in literature [14].

Table 1 Results of chemical analysis

Compound	Zn/%		C/%		H/%		N/%	
	calc.	found	calc.	found	calc.	found	calc.	found
$Zn(Hsal)_2(Him)_2$	13.81	13.8	50.72	49.7	3.38	3.8	11.82	11.5
$Zn(Hsal)_2(Him)_5$	9.62	9.6	51.21	51.1	4.41	4.4	20.60	20.0
$Zn(Hsal)_2(4\text{-}MeHim)_2$	12.98	12.5	52.68	51.1	3.98	4.7	11.12	10.9
$Zn(Hsal)_2(1,2\text{-}diMeim)_2$	12.30	12.3	54.22	53.7	4.89	4.9	10.54	10.1
$Zn(Him)_2$[a]	32.76	32.0	–	–	–	–	28.06	24.1
$Zn(4\text{-}MeHim)_2$[a]	27.70	28.4	42.21	44.5	4.40	4.5	24.62	19.3
$Zn(sal)(1,2\text{-}diMeim)$[a]	22.10	22.5	48.42	47.6	4.03	4.3	9.41	7.7

$Zn(Hsal)_2(Him)_2$ (a); $Zn(Hsal)_2(Him)_5$ (b); $Zn(Hsal)_2(4\text{-}MeHim)_2$ (c). A mixture of $ZnCO_3$, H_2sal, and imidazole or 4-methylimidazole in absolute ethanol was heated to 333 K, using magnetic stirring. The mixture was allowed to reflux for two hours (compound a and b) or for ten hours (compound c) and then the hot mixture was filtered. The obtained solutions were left to crystallize. The white precipitates were washed with ethanol (a, b). When the synthesis of (c) was carried out, oil was obtained. The oil was treated 5-fold with ether and the brownish precipitate was obtained. The reactions were carried out at different molar ratios: 1:2:3 (a), 1:2:5 (b) and 1:2:2 (c).

$Zn(Hsal)_2(1,2\text{-diMeim})_2$: $Zn(Hsal)_2\cdot 2H_2O$ was dissolved in a water solution of 1,2-dimethylimidazole (molar ratio 1:2). This procedure yielded a white precipitate. It was washed with water and dried at room temperature.

Chemical analysis

The zinc(II) was detected by complexometric titration with EDTA [15], while carbon, hydrogen, and nitrogen – by elemental analysis. The results are presented in Table 1.

X-ray analysis

Powder analysis

The X-ray analysis was carried out by means of a Siemens D 5000 powder diffractometer, using CuK_a radiation, 2θ range 2–80°. The products of synthesis and the sinters, formed as a result of thermal decomposition, were studied using X-ray method. Figure 1 presents powder diffraction patterns of $Zn(Hsal)_2(Him)_2$ and its sinters.

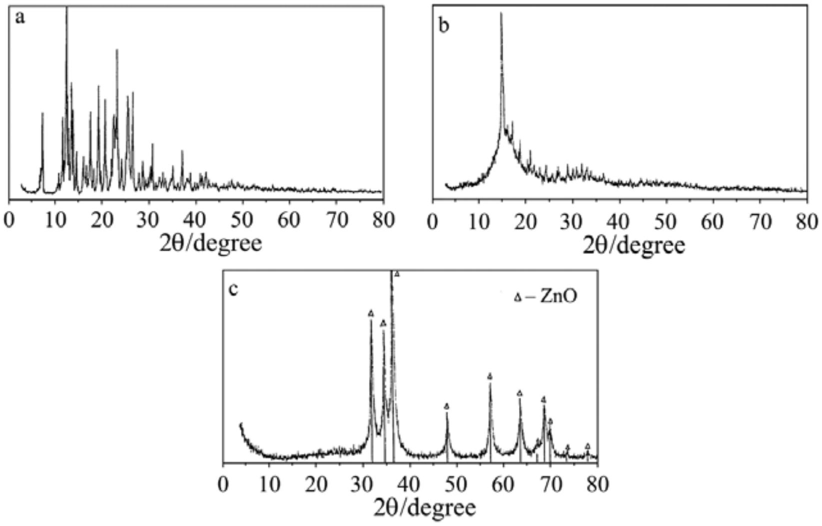

Fig. 1 X-ray analysis of $Zn(Hsal)_2(Him)_2$ complex: a – before sintering, b – after sintering at 653 K and c – after sintering at 973 K

X-ray structure analysis

Colorless crystals, suitable for X-ray experiment, were obtained only for $Zn(Hsal)_2(Him)_2$ and $Zn(Hsal)_2(1,2\text{-}diMeim)_2$ by slow evaporation of ethanol solutions. At first, both structures were solved based on X-ray experiment with CuK_α radiation (KM4 four-cycle diffractometer) and no absorption correction. MoK_α radiation was also used for $Zn(Hsal)_2(1,2\text{-}diMeim)_2$ analysis (KM4 four-cycle diffractometer with CCD camera). The structures were solved by direct methods using SHELXS97 [16] and refined with all data on F^2 using SHELXL97 [17]. All details of X-ray structure analysis are summarized in Table 2.

Table 2 Crystal data and summary of intensity data collection and structure refinement

	$Zn(Hsal)_2(Him)_2$	$Zn(Hsal)_2(1,2\text{-}diMeim)_2$	
		1	2
Empirical formula	$ZnC_{20}H_{18}N_4O_6$	$ZnC_{24}H_{26}N_4O_6$	$ZnC_{24}H_{26}N_4O_6$
Formula mass	475.75	531.86	531.86
Temperature/K	293(2)	293(2)	298(2)
Wavelength/Å	1.54178	1.54178	0.71073
Crystal system	tetragonal	orthorhombic	orthorhombic
Space group	$P\ 4_12_12$	$P\ 2_12_12_1$	$P\ 2_12_12_1$
a/Å	7.871(1)	8.030(2)	8.0110(16)
b/Å	7.871(1)	14.943(39	14.919(3)
c/Å	33.243(7)	20.863(4)	20.837(4)
Volume/$Å^3$	2059.5(6)	2503.4(9)	2490.4(9)
Z	4	4	4
Calculated density/mg m^{-3}	1.534	1.411	1.419
Absorption coefficient	2.062	1.755	1.032
F(000)	976	1104	1104
θ range/°	5.32 to 80.26	to 80.26	3.24 to 22.99
Index ranges	$-10<h<10$ $-9<k<0$ $0<l<42$	$0<h<9$ $0<k<19$ $0<l<26$	$-8<h<7$ $-16<k<16$ $-22<l<22$
Reflections collected/unique	4517/2254	2906/2881	13755/2789
Refinement method	F^2	F^2	F^2
Data/restraints/parameters	2254/0/143	2881/0/319	2789/0/317
Goodness-of-fit on F^2	1.156	1.535	1.130
R_1 indices $[I>2\sigma(I)]$	0.0549	0.0415	0.0711
wR_2	0.1209	0.4489	0.1181
Largest difference peak and hole/e $Å^{-3}$	0.973 and –1.179	3.36 and –0.69	0.351 and –0.496

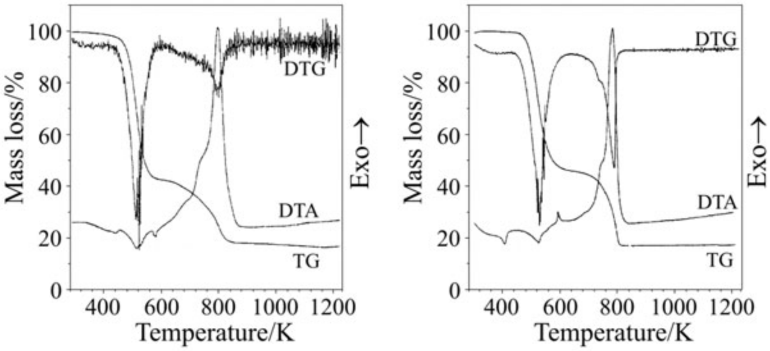

Fig. 2 Thermal curves of complexes

Thermal studies

The thermoanalytical measurements were carried out using a Balzers TG/DTA–SETSYS–16/18 thermoanalyzer with a Balzers mass spectrometer. The temperature range 293–1273 K; the heating rate 10 K min^{-1}, in air atmosphere; the sample mass <10 mg. The sinters were obtained on the basis of the TG curves. XRD and elemental analyses of the sinters were carried out (Table 3). The gaseous decomposition products of $Zn(Hsal)_2(Him)_2$ and $Zn(Hsal)_2(4\text{-}MeHim)_2$ complexes were analyzed. Figure 2 presents thermal curves of $Zn(Hsal)_2(Him)_2$ and $Zn(Hsal)_2(4\text{-}MeHim)_2$ as an example.

Results and discussion

The heteroligand complexes: $Zn(Hsal)_2(Him)_2$, $Zn(Hsal)_2(Him)_5$, $Zn(Hsal)_2(4\text{-}MeHim)_2$, and $Zn(Hsal)_2(1,2\text{-}diMeim)_2$ were obtained in the reaction of zinc salts with imidazole or its derivatives. Depending on the molar ratio of the reagents, two different mixed complexes were obtained for imidazole. The analysis of powder diffraction patterns showed that the three complexes have the crystalline structures, while 4-methylimidazole complex is amorphous.

X-ray structure analyses of $Zn(Hsal)_2(Him)_2$ and $Zn(Hsal)_2(1,2\text{-}diMeim)_2$ were conducted. Figure 3 shows the molecular units of the compounds $Zn(Hsal)_2(Him)_2$ and $Zn(Hsal)_2(1,2\text{-}diMeim)_2$. All selected geometrical details are gathered in Table 4. It should be mentioned that geometrical parameters for the structures of $Zn(Hsal)_2(1,2\text{-}diMeim)_2$, obtained by two methods, are comparable. However, the structure determined based on experiment with MoK_{α} radiation has better validation (Table 2). Therefore, in Table 4 and in subsequent discussion only the values obtained based on these data will be used. As it is clear from the Fig. 3, $Zn(Hsal)_2(Him)_2$ and $Zn(Hsal)_2(1,2\text{-}diMeim)_2$ consist of a Zn polyhedra (here tetrahedron). In both solved structures, the Zn ion is surrounded by two carboxylate groups, which are monodentate, and two imidazole or 1,2-dimethylimidazole molecules (Fig. 3). Hence, for full tetrahedron description, the two Zn–O and two Zn–N distances are essential. Half of chemical unit of

Table 3 Results of thermal analysis

Complex	Stage	Temperature/K	Formula	Mass loss/%		Peak nature	Temperature/ K
				calc.	found		
$Zn(Hsal)_2(Him)_2$	I	478–613	$Zn(im)_2$	57.86	58.0	endo	518
	II	683–953	ZnO	82.81	83.0	exo	813
$Zn(Hsal)_2(Him)_5$	I	fusion process				endo	353
	II	413–623	$Zn(im)_2$	70.43	69.0	endo	533
	III	693–903	ZnO	87.94	88.0	exo	843
$Zn(Hsal)_2(4\text{-}MeHim)_2$	I	fusion process				endo	403
	II	468–668	$Zn(4\text{-}Meim)_2$	54.6	53.5	endo	528
	III	723–903	ZnO	83.78	84.0	exo	823
$Zn(Hsal)_2(1,2\text{-}diMeim)_2$	I	fusion process				endo	453
	II	453–583	Zn(sal)(1,2-diMeim)	44.13	45.0	endo	568
	III	583–713	ZnO+org. fragm.	–	75.0	endo	663
	IV	440–550	ZnO	84.69	85.0	exo	768

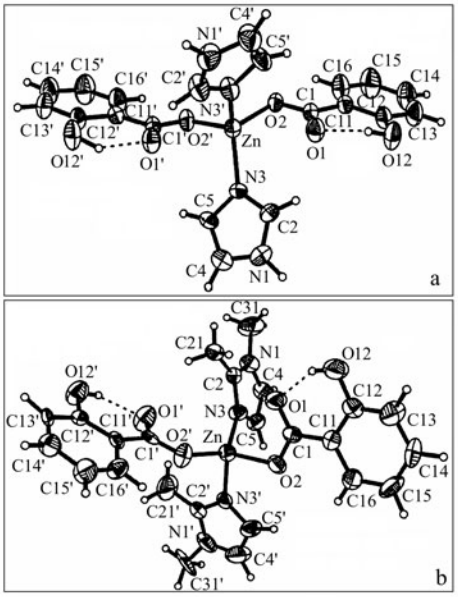

Fig. 3 Molecular structure of complexes: a – $Zn(Hsal)_2(Him)_2$ and b – $Zn(Hsal)_2(1,2\text{-diMeim})_2$

$Zn(Hsal)_2(Him)_2$ is crystallographically independent. From the data collected in Table 4, it is visible that Zn polyhedra coordination in two solved examples differs geometrically. In the structure of $Zn(Hsal)_2(Him)_2$ the Zn–O distance is significantly longer than the Zn–N one. But in the structure of $Zn(Hsal)_2(1,2\text{-diMeim})_2$ both Zn–N dis-

Table 4 Selected geometrical details for complexes. Bond length in Å and all angles in (°)

	$Zn(Hsal)_2(Him)_2$	$Zn(Hsal)_2(1,2\text{-diMeim})_2$	
		1	2
Zn-N3	1.985(2)	2.008(6)	2.035(3)
Zn-N3’	1.985(2)	1.978(6)	1.993(3)
Zn-O2	2.030(1)	1.990(5)	1.995(2)
Zn-O2’	2.030(1)	1.958(5)	1.959(2)
Zn-O1	2.700	2.911	2.889
Zn-O1’	–	3.078	3.057
N3-Zn-N3’	120.74(1)	104.4(2)	104.5(1)
N3-Zn-O2	104.90(7)	109.4(2)	109.3(1)
N3-Zn-O2’	–	128.8(2)	128.2(1)
N3’-Zn-O2’	–	106.3(2)	106.5(1)
O2-Zn-O2’	97.42(8)	105.2(2)	105.7(9)
O2-Zn-N3’	–	98.7(2)	98.9(1)
Zn-O2-C1-C11	168.82(0.17)	179.0(5)	–178.4(2)
Zn-O2’-C1’-C11’	–	178.3(5)	–176.8(2)
O12-H12A...O1	1.703	1.841	1.757
O12’-H12B...O1’	–	1.785	1.783

tances are longer than respective Zn–O ones. The 'reversing' of these distances lengths reflects on the values of bond angles formed by Zn with respective O and/or N (Table 4). The volume of substituted and unsubstituted imidazole differs significantly. Therefore, space filled by two methyl substituents reflects on pulling up imidazole moiety and enlarging the Zn–N distances in $\mathrm{Zn(Hsal)_2(1,2\text{-}diMeim)_2}$. At the same time, oxygen atoms are coming nearer to Zn to fill out added free space. It reflects on stretching the torsion angles of Zn-O2-C1-C11 and on increasing the distances between Zn and the second carboxy-oxygen in $\mathrm{Zn(Hsal)_2(1,2\text{-}diMeim)_2}$ in comparison with the structure of $\mathrm{Zn(Hsal)_2(Him)_2}$. Additionally, in $\mathrm{Zn(Hsal)_2(1,2\text{-}diMeim)_2}$, the size of 1,2-dimethylimidazole ligand is responsible for the difference between two analogical bonds Zn–N and two analogical bonds Zn–O. In both structures under discussion, crystals include isolated chemical units. However, in such units two intramolecular hydrogen bonds $\mathrm{O12\text{-}H12A\cdots O1}$ and $\mathrm{O12'\text{-}H12B\cdots O1'}$ were identified. In the structure of $\mathrm{Zn(Hsal)_2(Him)_2}$, mentioned above H-bonds are stronger than those in $\mathrm{Zn(Hsal)_2(1,2\text{-}diMeim)_2}$ (Table 4).

The mass loss, the chemical and powder diffractometric analysis of the sinters, endo- and exothermic effects indicate that the strength of bond between the metal and ligand determines the course of thermal decompositions for all the complexes.

In the pyrolysis of the $\mathrm{Zn(Hsal)_2(Him)_2}$ and $\mathrm{Zn(Hsal)_2(4\text{-}MeHim)_2}$ two molecules of *o*-hydroxybenzoic acid are lost at first. The chemical analysis indicated that the sinters have formulae: $\mathrm{Zn(im)_2}$ and $\mathrm{Zn(4\text{-}Meim)_2}$. Their diffractograms are different from diffractograms of initial compounds (e.g. Figs 1a and 1b). Inorganic compound (ZnO) forms in the next stage (Fig. 1c). Thermal decomposition of the compounds named above proceeds in accordance with reactions I and II:

$$\mathrm{Zn(Hsal)_2(Him)_2 \rightarrow Zn(im)_2 \rightarrow ZnO} \qquad \text{(I)}$$

$$\mathrm{Zn(Hsal)_2(4\text{-}MeHim)_2 \rightarrow fusion\ process \rightarrow Zn(4\text{-}Meim)_2 \rightarrow ZnO} \qquad \text{(II)}$$

The analysis of the gaseous products of decomposition of $\mathrm{Zn(Hsal)_2(Him)_2}$ confirmed the emission of the *o*-hydroxybenzoic acid molecules. The ionic current that originates from emission of acid (molecular ion m/z 138), phenol, and benzene (fragment ions m/z 92 and 78, 77, 52, 51, 50) increases at the first stage temperature range. Since the amount of nitrogen in the 613 K sinters is equal to 24.1% (theor. in $\mathrm{Zn(im)_2}$ – 28.06%), it is assumed that also some imidazole evaporates in the first stage (fragment ion m/z 68). The complete decomposition of the $\mathrm{Zn(im)_2}$ takes place in the second stage. Then, the gaseous products include mostly NO (m/z 30), CO_2 (m/z 44) and H_2O (m/z 18). Analogous gaseous products are generated in the case of decomposition of the 4-methylimidazole complex, and the ionic current from emission of CH_3 group does not increase till the second stage. This is confirmed by the formation of $\mathrm{Zn(4\text{-}Meim)_2}$ in the stage after fusion process.

The decomposition of the $\mathrm{Zn(Hsal)_2(Him)_5}$ complex proceeds in three stages. The course of the thermal curves indicates that there is the endothermic peak at 353 K and no mass loss in the first stage. In the second stage zinc complex decomposes to $\mathrm{Zn(im)_2}$. The final product of the decomposition is zinc oxide (Table 3, reaction III).

$$\mathrm{Zn(Hsal)_2(Him)_5} \rightarrow \text{fusion process} \rightarrow \mathrm{Zn(im)_2} \rightarrow \mathrm{ZnO} \tag{III}$$

Also the pyrolysis of $Zn(Hsal)_2(1,2\text{-diMeim})_2$ complex begins with the phase transition (endothermic peak at 453 K). The next stages proceed with the gradual mass loss. In the second stage, one molecule of the 1,2-dimethylimidazole and one molecule of the *o*-hydroxybenzoic acid are lost. Zn(sal)(1,2-diMeim) is the product of this reaction. The diffractometric analysis showed that zinc oxide forms in the third stage of decomposition together with organic fragments of the ligands. The pure zinc oxide is the product of the fourth stage. (Table 3, reaction IV).

$$\mathrm{Zn(Hsal)_2(1,2\text{-}diMeim)_2} \rightarrow \genfrac{}{}{0pt}{}{\text{fusion}}{\text{process}} \rightarrow \mathrm{Zn(sal)(1,2\text{-}diMeim)} \rightarrow \mathrm{ZnO} + \genfrac{}{}{0pt}{}{\text{organ.}}{\text{fragm.}} \rightarrow \mathrm{ZnO} \tag{IV}$$

The course of the pyrolysis (in conditions determined in this paper) and molecular structures of $Zn(Hsal)_2(Him)_2$ and $Zn(Hsal)_2(1,2\text{-diMeim})_2$ lead to the same conclusions about the strength of zinc-imidazole or 1,2-dimethylimidazole and zinc-*o*-hydroxybenzoate bonds.

The thermal stability of the compounds decreases in the following order:

$$\begin{array}{lllll} & \mathrm{Zn(Hsal)_2(Him)_2} > & \mathrm{Zn(Hsal)_2(4\text{-}MeHim)_2} > & \mathrm{Zn(Hsal)_2(1,2\text{-}diMeim)_2} > & \mathrm{Zn(Hsal)_2(Him)_5} \\ T_\mathrm{i} = & 478\ \mathrm{K} & 468\ \mathrm{K} & 453\ \mathrm{K} & 418\ \mathrm{K} \end{array}$$

where T_i – initial temperature of decomposition.

Conclusions

- The composition of di(*o*-hydroxybenzoate)zinc(II) complexes with imidazole depends on molar ratio reagents, but that of complexes with derivatives of imidazole does not. Compounds with imidazole and 1,2-dimethylimidazole have a crystalline structure, while compound with 4-methylimidazole is amorphous.
- Thermal decomposition of the mixed complexes has a multi-stage course. The complex containing imidazole is thermally most stable from among the complexes of the same generalized formula $Zn(A)_2(B)_2$ (where A – $Hsal^-$; B – Him, 4-MeHim, 1,2-diMeim).
- The course of pyrolysis (in conditions determined in this paper) and molecular structure of the complexes lead to the same conclusions about the strength metal-ligand bonds.
- Zinc oxide is the final pyrolysis product of all the investigated complexes.
- $Zn(Hsal)_2(Him)_2$ and $Zn(Hsal)_2(1,2\text{-diMeim})_2$ have the tetrahedron structure. Metal is surrounded by two monodentate carboxylate groups and two imidazole or
- 1,2-dimethylimidazole molecules. In $Zn(Hsal)_2(Him)_2$ complex, the Zn–N bonds are stronger than the Zn–O bonds, in $Zn(Hsal)_2(1,2\text{-diMeim})_2$ the inverse of bond strength is observed.
- In $Zn(Hsal)_2(1,2\text{-diMeim})_2$ every *o*-hydroxybenzoate ion and every 1,2-dimethylimidazole molecule are differently bound by zinc. We encounter two different Zn–N bonds as well as two different Zn–O bonds.

- Intramolecular hydrogen bonds are found in both investigated structures. These bonds are stronger in $Zn(Hsal)_2(Him)_2$ than those in $(Hsal)_2(1,2\text{-diMeim})_2$.

References

1 M. Olczak-Kobza, Thermochim. Acta, 366 (2001) 129.
2 A. Turek and M. Olczak-Kobza, J. Therm. Anal. Cal., 54 (1998) 133.
3 M. Olczak-Kobza, Polish. J. Chem., 69 (1995) 1396.
4 M. Olczak-Kobza, J. Therm. Anal. Cal., 55 (1999) 989.
5 M. Olczak-Kobza and M. Cichecka, J. Therm. Anal. Cal., 66 (2001) 1379.
6 B. Lenarcik and K. Kurdziel, Pol. J. Chem., 55 (1981) 737.
7 B. Lenarcik and B. Barszcz, J. Chem. Soc., Dalton Trans., (1984) 27.
8 J. Reedijk, Rec. Trav. Chim., 88 (1969) 1451.
9 R. N. Patel, H. C. Panday, K. B. Pandaya and G. N. Mukherjee, Ind. J. Chem., 38(A) (1999) 850.
10 W. D. Horrocks, J. N. Ishley and R. R. Whittle, Inorg. Chem., 21 (1982) 3265, 3270.
11 N. M. Sivasankarani, S. Jawaharunnissa and L. Kamakshi, Ind. J. Chem., 29A (1990) 581.
12 R. N. Patel, R. P. Srivastawa, N. Singh, S. Kumar and K. B. Pandeya, Ind. J. Chem., 40A (2001) 361.
13 A. Busnot, F. Busnot, J. F. Hemiday and J. F. LeQuerler, Thermochim. Acta, 228 (1993) 219.
14 K. Rissanen, J. Valkonen, P. Kakkonen and M. Leskele, Acta Chem. Scand., A 41 (1987) 299.
15 A. Cygański, 'Chemiczne metody analizy ilo'sciowej', WNT, Warszawa 1999, p. 526.
16 G. M. Sheldrick, SHELXS97, University of Gottingen, Germany 1997.
17 G. M. Sheldrick, SHELXS97, University of Gottingen, Germany 1997.